

COPY 3

Report No. FAA-RD-73-40 -49

APR 30 1973

NAFEC
LIBRARY

490A-92
182

AIR-TO-AIR VISUAL DETECTION DATA

PART I-Summary of Air-To-Air Visual Detection Data

Mr. A. Millhollon, SRDS

PART II-Summary of Visual Detection Data

Mr. J. Lyons, Control Data Corp.

PART III-Summary of Visual Detection Data Taken

During The ATA/CAS Flight Tests

Mr. W. Graham, Control Data Corp.



April 1973

INTERIM REPORT

Document is available to the public through the
National Technical Information Service,
Springfield, Virginia 22151

**DEPARTMENT OF TRANSPORTATION
FEDERAL AVIATION ADMINISTRATION
Systems Research & Development Service
Washington, D.C. 20591**

This document is disseminated under the sponsorship of the Department of Transportation in the interest of information exchange. The United States Government assumes no liability for its contents or use thereof.

1. Report No. FAA-RD-73-40	2. Government Accession No.	3. Recipient's Catalog No.	
4. Title and Subtitle AIR-TO-AIR VISUAL DETECTION DATA		5. Report Date April 1973	
		6. Performing Organization Code	
7. Author(s) A. Millhollon, J. Lyons, W. Graham		8. Performing Organization Report No.	
9. Performing Organization Name and Address Control Data Corp. Advanced Studies Laboratory 4201 Lexington Ave., North St. Paul, Minnesota		10. Work Unit No. (TRAIS) 051-241	
		11. Contract or Grant No. DOT-FA70WA-2263	
12. Sponsoring Agency Name and Address Department of Transportation Federal Aviation Administration Systems Research and Development Service Washington, D. C. 20591		13. Type of Report and Period Covered Interim Report	
		14. Sponsoring Agency Code	
15. Supplementary Notes			
16. Abstract Since the pilot is required to visually detect potentially hazardous intruders in the Pilot Warning Instrument (PWI) concept, the question of pilot air-to-air visual detection is critical. The significant conclusion from the data presented in this report is that under good Visual Flight Rule (VFR) conditions, if the pilot is given accurate information on the location of intruding aircraft he has a high likelihood of seeing the intruder in sufficient time to take any required evasive action. This report presents two Control Data Corp. (CDC) papers summarizing data from two different air-to-air visual detection activities.			
17. Key Words Visual Detection Pilot Warning Instrument Air-to-Air Data		18. Distribution Statement Document is available to the public through the National Technical Information Service, Springfield, Virginia 22151	
19. Security Classif. (of this report) UNCLASSIFIED	20. Security Classif. (of this page) UNCLASSIFIED	21. No. of Pages 38	22. Price 3.00 PC .95 MF

PART I

SUMMARY OF AIR-TO-AIR VISUAL DETECTION DATA

BY
MR. A. MILLHOLLON
FEDERAL AVIATION ADMINISTRATION/SYSTEMS RESEARCH AND DEVELOPMENT SERVICE
WASHINGTON, D. C.

Introduction: The purpose of this report is to present two Control Data Corporation (CDC) papers summarizing air-to-air visual detection data. This report is in three parts with Part I containing introductory remarks and Parts II and III being copies of the original CDC papers by Mr. J. Lyons, and Mr. W. Graham. The data from these papers are an output of the Federal Aviation Administration's Pilot Warning Instrument (PWI) program, under the CDC contract DOT-FA70WA-2263.

Since the pilot is required to visually detect potentially hazardous intruders in the PWI concept, the question of visual detection is critical. The significant conclusion from the data presented in this report is that under good Visual Flight Rule (VFR) conditions, if the pilot is given accurate information on the location of intruding aircraft he has a high likelihood of seeing the intruder in sufficient time to take any required evasive action.

Discussion: Of the several concepts being considered to reduce the hazard of mid-air collisions, the Collision Avoidance System (CAS) is probably the best known. The CAS is an Instrument Flight Rules (IFR) device. In operation it detects the intruding aircraft and, through pre-arranged logic, displays to the pilot (in a timely manner) the evasive maneuver he should make. With the CAS, the pilot does not necessarily see the intruder he is avoiding. On the other hand the PWI is a VFR device that locates the

intruding aircraft and indicates to the pilot where to look to find the intruder. It is then up to the pilot to assess the threat and take the necessary evasive action. For this reason, the ability of the pilot to visually detect other aircraft is a critical factor in the success of a PWI as a collision prevention aid. During 1969, 1971, and 1972 the FAA had the opportunity to collect visual detection data from two flight missions. The first opportunity occurred when the Air Transport Association (ATA) contracted with the Martin-Marietta Corp., Baltimore, Md., to flight test experimental CAS equipments. The second opportunity occurred when the CDC conducted near-miss photographic missions at the FAA's National Aviation Facilities Experimental Center (NAFEC) Atlantic City, N. J. In each of these missions two or more aircraft were controlled to fly near-miss encounters. It should be noted that PWI equipment was not installed in either aircraft. In the ATA tests, the pilot, copilot, and observer were maintaining a visual search for the target aircraft. For the photographic missions run by CDC, an observer (safety copilot) was visually searching for the target aircraft. The paper in Part II of this report summarizes the visual detection data taken during the NAFEC photographic mission. The paper in Part III of this report summarizes the visual detection data taken during the ATA CAS tests.

The Lyons paper presented in Part II of this report contains approximately 280 data points. As mentioned earlier, these data were taken during the air-to-air photographic missions (typical mission Part I Fig. 1) completed at NAFEC in February 1972. For this mission the desire and procedures for collecting visual detection data were recognized; consequently, the data

sample is larger and probably more accurate. The raw data from these missions are shown on Tables 1A through 1B, Tables 2A, through 2D, and Table 3. Tables 4, 5, and 6 show the cumulative probability points derived from the raw data. Figs. 1, 2, and 3 are simple plots of the data from Tables 4, 5, and 6. At this point it is well to turn to Part III, Figure 2 of the W. Graham paper. The smooth curves on Fig. 2 are representative averages from Part II, Figs. 1, 2, and 3. They were put together to provide a quick comparison of the detection range characteristics for various aircraft and closing speeds. To assist in interpreting these data, detection ranges were converted to "Time to Closest Approach" by dividing the detection range by the closing velocity for that specific encounter geometry. While this calculation is only valid for zero miss distances the results are accurate enough to provide an estimate of the time available to a pilot to assess a threat and take evasive action if necessary. Part I, Fig. 3 presents the cumulative probability of detection curves with an abscissa scale in seconds.

The visual detection data from the ATA CAS flight tests were collected during the summer and fall of 1969. Approximately 40 observations are recorded in the W. Graham paper (Part III). The raw data are listed in Table 1 and the cumulative probability of detection derived from those data are shown as the stair step curves in Figure 2. To give the reader some insight into a typical aircraft encounter flight a sample test run is shown in Part I, Figure 2. A primary point of interest common to all these data is that the pilot in all cases was given information on the location of the intruding aircraft. This information was based on radar

tracking and in some cases based on the CAS equipment range and range rate readings. An assumption applied at this point is that such information approximates the performance of a moderate grade PWI. Therefore, these data imply an estimate of the pilot assistance offered by a moderate performance PWI system.

Conclusion: The reader is cautioned about deriving firm conclusions from these data since there were limitations in running these experiments. There was a small cross section of observers which may not accurately represent the pilot population. The location information given each observer is not necessarily representative of a practical PWI. The observer workload level probably was not typical. No false alarms were given. Traffic conditions were light. All tests were conducted when visibility was five miles or greater (good VFR as opposed to marginal VFR).

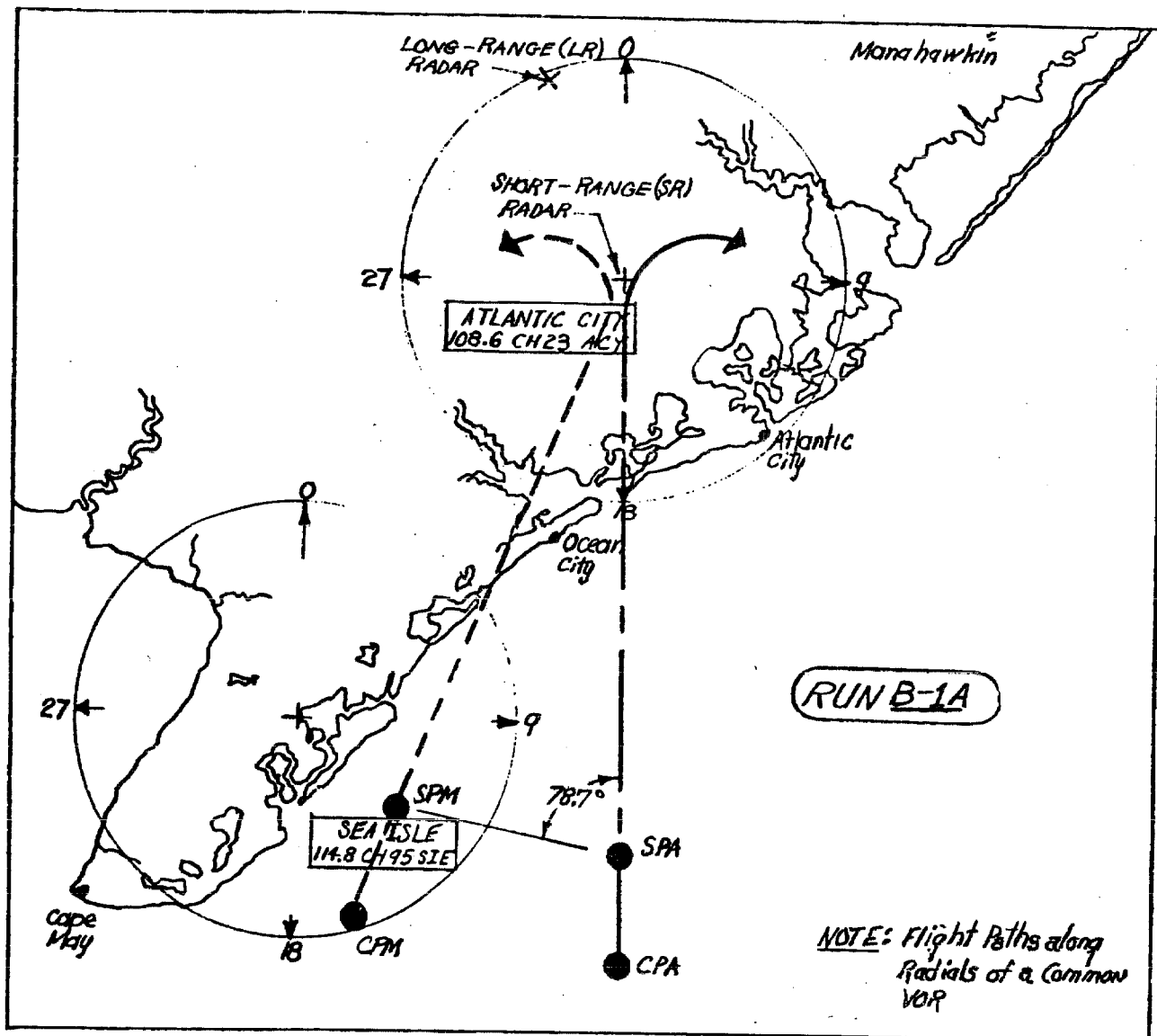
In spite of the above limitations, the data included herein give an indication of the potential performance of pilots aided by a PWI. It is encouraging to note in Part I, Fig. 3 that for all aircraft with the exception of the Jet Star a pilot had on the order of 20 to 50 seconds minimum and 50 to 90 seconds average to make an evasive maneuver when given representative "PWI" information.

As would be expected, larger aircraft, given the same closing speed as a small aircraft, were more readily detectable. For small, fast jets in head-on encounters there was a significant probability that even with PWI information the pilot did not see the intruder, as evidenced by the maximum cumulative probability of 0.82 at zero time. However, we do not

5

have a record of the miss distance, and this figure may be pessimistic. In cases where the observer did see the small jet his average time to react was 30 seconds.

Using these data as a check, the FAA PWI program will include several visual detection simulation experiments at the Department of Transportation's Transportation Systems Center (TSC), Cambridge, Mass. It is expected that the limitations described above can be evaluated during these simulations and that final data representative of practical PWI/Pilot situations will result. With these data, it is expected that the FAA can closely estimate the benefit which can be derived from various PWI systems.



RUN PARAMETERS
Relative Velocity: $V_R = 46.3$ knots, IAS
Relative Heading: $\alpha = 22.5$ Degrees
Miss Distance: $D = 0$ Feet
Film Time: $T_{10} = 11.6$ Min
No. of A/C Slides: $N = 18$

AZTEC PARAMETERS
Flight Path: — — — — —
Heading: 0 Degrees
Airspeed: 120 knots, IAS
Altitude: To be specified at flight-time.
Checkpoint A: VOR ACT --- 180° DME ACT --- 30.5 nm
Starting Point A: SR Radar Range - 26 nm SR Radar Az --- 180°
LR Radar Range - 35 nm LR Radar Az --- 174.5°

MUSKETEER PARAMETERS
Flight Path: — — — — —
Heading: 22.5 Degrees
Airspeed: 120 knots, IAS
Altitude: To be specified at flight-time.
Checkpoint M: VOR ACT --- 202.5° VOR SIE --- 162.5°
Starting Point M: SR Radar Range - 26 nm SR Radar Az --- 202.5°
LR Radar Range - 34 nm LR Radar Az --- 191.5°

FIGURE 1
TYPICAL CONTROLLED NEAR-MISS FLIGHT PLAN
(NAFEC PHOTOGRAPHIC MISSION)

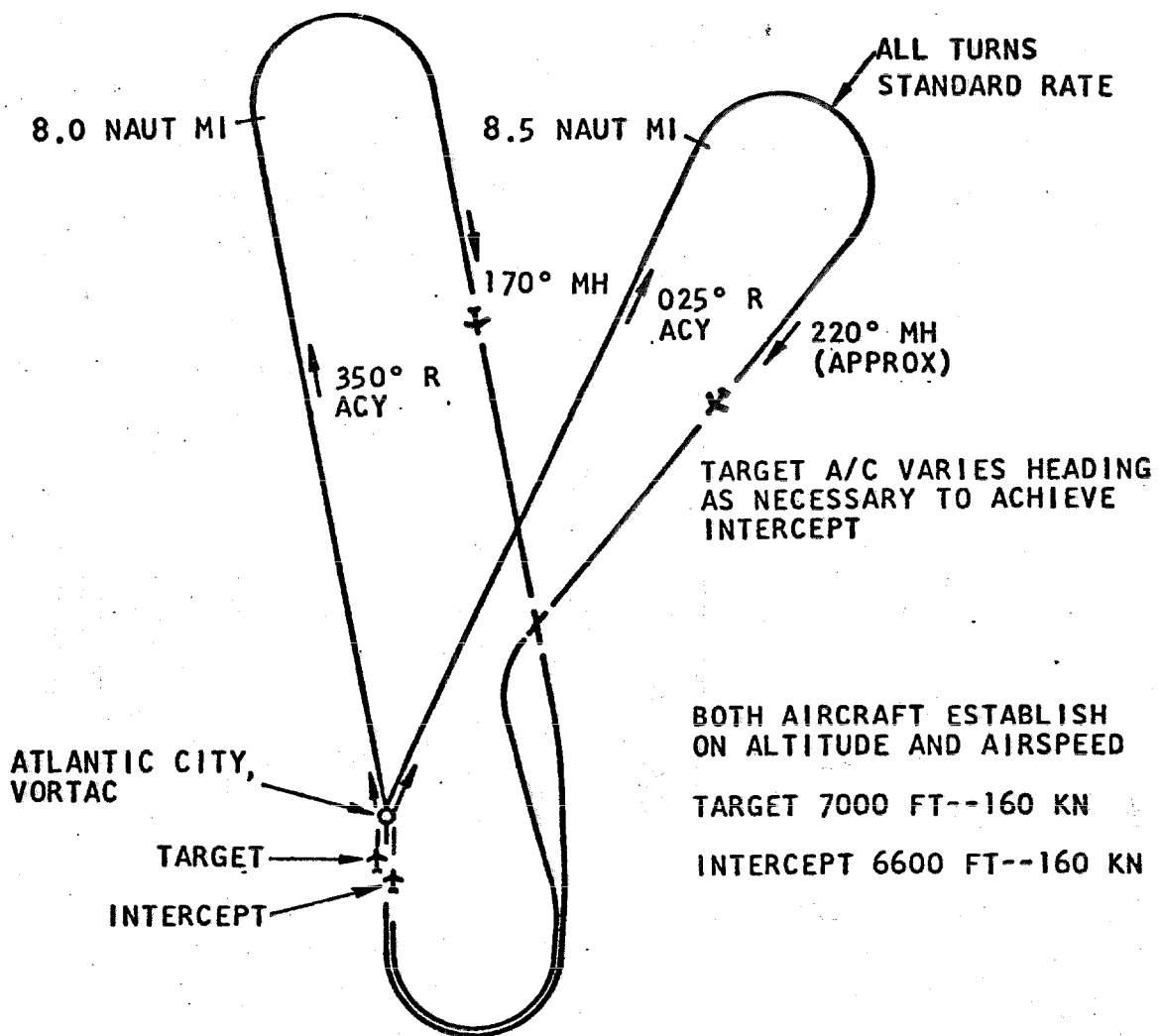


FIGURE 2

TYPICAL CONTROLLED NEAR-MISS FLIGHT PLAN

(ATA CAS/TESTS)

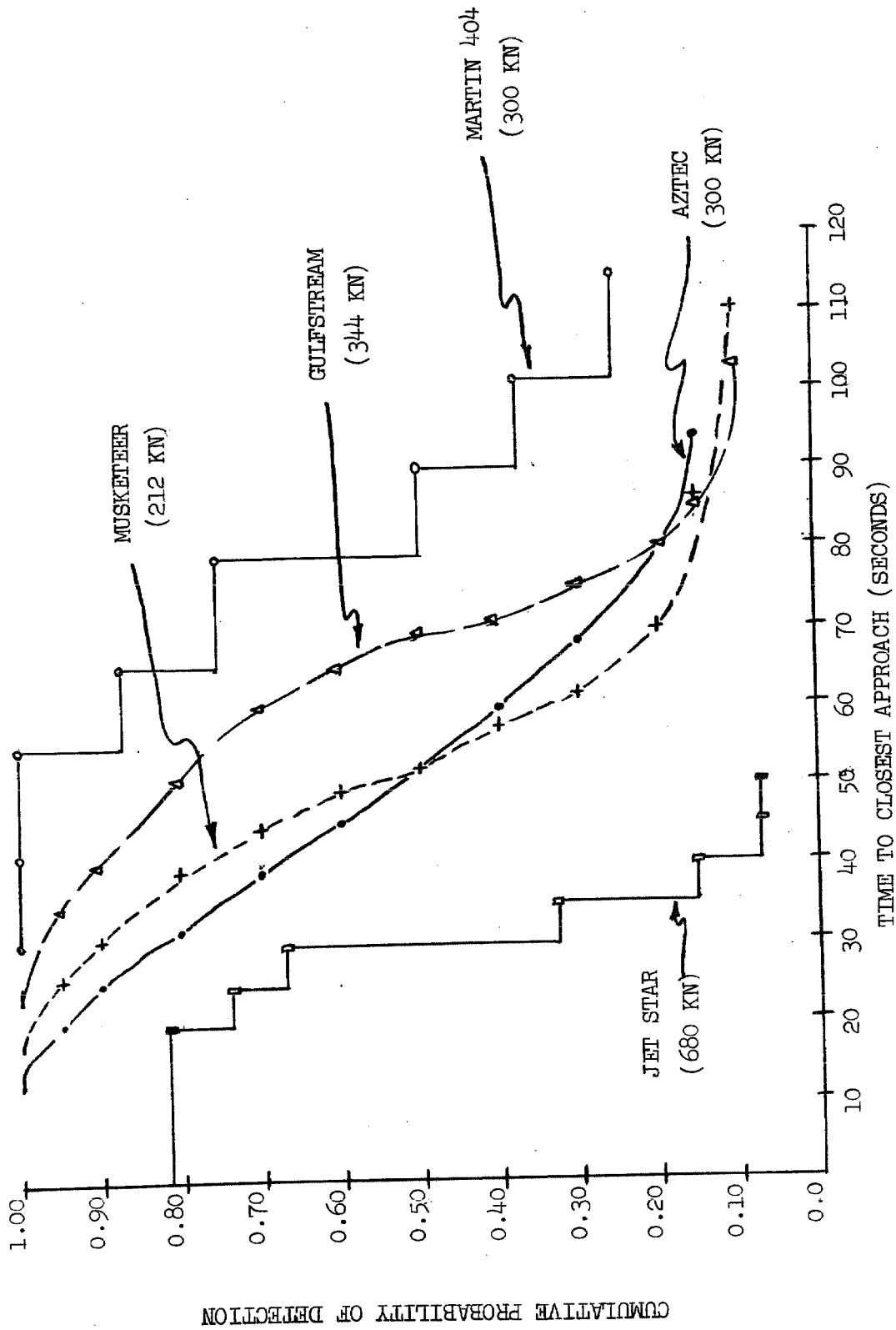


FIGURE 3
 CUMULATIVE PROBABILITY OF DETECTION
 V.S. TIME TO CLOSEST APPROACH
 (FOR VARIOUS CLOSING SPEEDS & TYPES OF AIRCRAFT)

PART II

SUMMARY OF VISUAL DETECTION DATA

Report No. CDC-JL-5

Contract No. DOT-FA-70WA-2263

Mr. J. Lyons
Control Data Corporation

Submitted to:

Federal Aviation Administration
800 Independence Avenue
Washington, D. C.

Submitted by:

Control Data Corporation
Advance Systems Laboratory
Saint Paul, Minnesota

Date: 18 March 1972

Author: J. Lyons

INTRODUCTION

One task on this contract has been to design and photograph flights at NAFEC to obtain film for a later simulation. These flights, which were completed in mid February, 1972, included 150 missions during which two aircraft set out on collision and near-miss courses. In addition to the photography in each run, we also recorded the time and range of first visual detection of each aircraft by the crew of the other aircraft. The note below summarizes this data in tables and figures.

NOTES

1. In the tables NC signifies no visual contact during that run, NR means we have no reliable data, RVD denotes the estimated range of first visual detection, D indicates the estimated miss distance, and S,R denotes the flight and film Set/Run.
2. The indicated run codes refer to specific encounter geometries which are described in another report.*
3. In all runs, detection in the Aztec was by the co-pilot who had no other workload.
4. In each aircraft the crew was informed of the run geometry and the clock position of the other aircraft.
5. Approximately 80% of the runs were conducted under scattered clouds with visibility in excess of 10 miles.
6. For the curves of detection probability, we used only those cases for which $R_{VD} \geq 2D$.
7. All runs were designed with the Musketeer (the target aircraft) within the 9:00 to 12:00 o'clock sector of the Aztec (the camera aircraft). With respect to the Musketeer, the Aztec position varied from 12:00 to 6:00.

* Lyons, J., "Phase II Photographic Flight Plan", Control Data Corporation, Report No. CDC-JL-5 under Contract No. DOT-FA-70WA-2263.

8. In all runs the aircraft were separated by 500 feet in altitude.
9. Although many variable factors influenced the visual detection ranges, we have made no attempt to isolate these factors and correlate them with the results. We list the major factors below:
 - (a) Flight profiles were selected to ensure that the sun was not within the field-of-view of the camera, and this also ensured that it never appeared in the vicinity of the Musketeer clock position. The reverse was not true and the Musketeer on several occasions had to search for the Aztec in the vicinity of the sun.
 - (b) The Aztec was more detectable against a white cloud background than against an ocean background. The reverse was true for the Musketeer. (About half of the runs were conducted with the Aztec above the Musketeer.)
 - (c) The Aztec was often at unfavorable clock positions (3:00 to 6:00) for detection by the pilot in the Musketeer.
 - (d) There was considerable variation in the vision of four different co-pilots in the Aztec.
 - (e) With winds the crab angle in the Musketeer altered the clock position at which he could expect to observe the Aztec. This was not the case with the Aztec because our flight control always maintained the Musketeer at the correct clock position with respect to the Aztec heading.
10. Tables 1, 2, and 3 give the estimated range at the time of first detection, RVD. Tables 4, 5, and 6 show the calculation of the cumulative probability of first detection, P_D , as a function of range. This probability gives the percent of targets which were detected by a given range. The runs have been divided into groups based on closing speed in making this calculation. Consider as an example the left hand block in table 4 which summarizes detection of the Musketeer by the co-pilot of the Aztec for the 21 runs with closing speed in the interval 33 - 100 knots (and with relative heading in the interval 0 - 45°). The Musketeer was detected in everyone of the 21 runs so the cumulative probability of detection reaches unity at the

smallest range of first detection, 1.2 nmi. The greatest range at which the target was first detected was 8.9 nmi at which point the cumulative probability of detection equals $1/21 = 0.048$; that is, one of the 21 targets was first detected at this range. Another target was first detected at 8.0 nmi, so that two targets were detected by this range; therefore, $P_D = 2/21 = 0.095$, etc. Figures 1, 2, and 3 present these data as smoothed curves and illustrate the general result that the cumulative probability of detection decreases with increasing closing speed.

RUN CODE	V _R KNOTS	α DEGREES	S,R RVD D	S,R RVD D	S,R RVD D	S,R RVD D	S,R RVD D	S,R RVD D	S,R RVD D	S,R RVD D	S,R RVD D	S,R RVD D	S,R RVD D
A-2A	33	0	10,4 1.2 0.4	18,1 2.0 0.3	22,1 2.9 0.8								
A-5A	33	0											
B-1A	51	22.5	4,1 2.5 0.1	4,4 1.5 NR	13,7 3.8 0.7	14,1 2.8 0.2	18,2 6.3 0.2						
B-2A	51	22.5	14,2 4.3 3.3										
B-7A	51	22.5	7,5 6.1 2.0	7,6 7.7 1.8	19,1 3.8 0.2								
C-1A	63	22.5	2,1 1.0 0.8	2,4 8.2 NR	8,1 2.8 0.3	8,2 3.1 0.1	19,2 3.7 0.3						
C-6A	63	22.5	6,1 8.0 1.0	6,5 6.0 4.7	6,7 3.4 0.6	10,3 8.9 0.2							
D-1A	101	45	5,6 1.8 0.3	5,11 2.0 0.4	14,3 3.7 0.2	15,6 5.9 1.5	22,7 3.0 0.2						
E-1A	110	45	3,1 6.0 0.5	3,5 5.0 0.9	20,4 1.9 0.2	22,2 3.8 0.2							

TABLE 1A
DETECTION OF MUSKETEER BY CO-PILOT IN AZTEC

RUN CODE	V _R KNOTS	α DEGREES	S,R RVD D	S,R RVD D	S,R RVD D								
E-2A	110	45	9,1 3.8 3.0	10,2 3.1 0.2									
E-6A	110	45	14,4 1.9 0.1										
E-7A	110	45	6,2 6.7 3.6	6,8 6.7 2.2									
F-1A,B	147	67.5	4,3 0.9 0.3	4,6 0.9 0	9,4 NC 2.3	9,5 2.2 1.5	12,3 3.7 0.1	13,1 2.9 0.3					
F-7A	147	67.5	18,3 4.3 1.3										
G-1A	156	67.5	3,2 5.2 0.5	3,6 2.5 0.5	17,5 4.0 0.5	19,3 3.6 0.5							
G-2A	156	67.5	19,4 2.5 0.2										
G-7A	156	67.5	7,7 NC 1.6	7,8 4.0 4.0	18,4 1.4 1.3								
H-1A	187	90	5,1 3.7 0.3	5,2 1.7 0.2	9,8 3.3 1.0	9,9 3.1 1.3	9,10 4.1 0.3	12,4 3.5 0.3	13,2 2.3 0.2	20,5 2.9 0.2	21,6 3.8 0.1		

TABLE 1B
DETECTION OF MUSKETEER BY CO-PILOT IN AZTEC

RUN CODE	V _R KNOTS	α DEGREES	S,R RVD D	S,R RVD D	S,R RVD D	S,R RVD D							
H-5A	187	90	10,1 1.5 0.8										
H-7A	187	90	7,9 2.6 1.2	7,10 NC 1.4									
I-1A	196	90	2,2 2.0 NR	2,5 9.9 2.9	8,7 3.0 0	8,8 1.0 0.5	15,7 3.0 0.5						
I-7A	196	90	6,3 7.6 1.4	6,6 4.3 1.7									
J-1A	219	112.5	5,3 2.1 0.4	5,4 2.6 0.4	12,1 1.8 0.5	17,6 0.9 0.5	19,5 2.0 0.8						
J-7A	219	112.5	9,11 2.8 2.0	16,5 0.9 0.7									
K-1A	229	112.5	3,3 1.9 0.5	3,7 3.7 0.3	13,3 NC 0.9	13,4 0.7 0.5	17,7 3.0 1.0	17,8 2.0 1.5	19,7 1.0 0.8	19,8 1.5 1.2	20,6 NC 1.0	21,8 2.3 0.2	
K-6A	229	112.5	7,1 NC 1.6	7,2 2.4 1.4	11,2 NC 1.4								
L-1A	243	135	4,2 1.2 0.3	4,5 1.5 1.2	5,9 0.5 0.5	5,10 0.5 0.3	14,5 1.3 0.6	16,6 0.8 0.5					

TABLE 1C
DETECTION OF MUSKETEER BY CO-PILOT IN AZTEC

RUN CODE	V _R KNOTS	∠ DEGREES	S,R RVD D	S,R RVD D	S,R RVD D								
L-7A	243	135	7,3 NC 1.5	7,4 5.5 1.5	11,3 2.5 2.5	11,4 3.0 NR	11,5 4.8 1.0						
M-1A	254	135	3,4 4.0 1.5	16,7 1.0 1.0	18,5 1.9 0.1	21,9 1.2 0.5							
N-1A	259	157.5	5,7 NC 1.0	5,8 1.0 0.9	8,3 0.3 0.3	8,4 0.5 0.2	12,2 2.0 1.2	13,5 1.4 1.1	13,6 4.3 0.9	19,6 1.0 0.2	21,10 1.0 0.2	22,3 1.5 0.3	22,4 2.2 0.2
O-1A	270	157.5	2,3 NR 0.5	8,5 1.0 0.3	8,6 4.0 0.2	20,1 1.6 0.2							
O-4A	270	157.5	6,4 NC 4.2	20,2 1.2 0.9									
O-7A	270	157.5	20,3 1.8 1.1										
O-8A	270	157.5	9,6 2.9 2.9	9,7 NC 4.5	12,5 NC 3.6	12,6 NC 3.0							
Q-4A	275	180	9,2 2.1 2.1	9,3 5.8 3.1	22,5 NC 0.5	22,6 0.5 0.4							

TABLE 1D
DETECTION OF MUSKETEER BY CO-PILOT IN AZTEC

RUN CODE	V _R KNOTS	α DEGREES	S,R RVD D	S,R RVD D	S,R RVD D	S,R RVD D	S,R RVD D	S,R RVD D	S,R RVD D				
A-2A	33	0	10,4 1.3 0.4	18,1 1.5 0.3	22,1 1.0 0.8								
B-1A	51	22.5	4,1 1.5 0.1	4,4 NR NR	13,7 3.9 0.7	14,1 2.3 0.2	18,2 1.3 0.2						
B-2A	51	22.5	14,2 4.3 3.3										
B-7A	51	22.5	7,5 5.1 2.0	7,6 3.8 1.8	19,1 5.6 0.2								
C-1A	63	22.5	2,1 NR 0.8	2,4 8.4 NR	8,1 2.1 0.2	8,2 6.5 0.1	19,2 4.8 0.3						
C-6A	63	22.5	6,1 2.4 1.0	6,5 NC 4.7	6,7 3.4 0.5	10,3 8.5 0.2							
D-1A	101	45	5,6 1.8 0.3	5,11 6.0 0.3	14,3 2.4 0.2	15,6 NC 1.5	22,7 6.0 0.2						
E-1A	110	45	3,1 1.5 0.5	3,5 3.0 0.8	20,4 4.5 0.2	22,2 4.6 0.2							
E-2A	110	45	9,1 4.2 3.0	10,2 4.0 0.2									

TABLE 2A
DETECTION OF AZTEC BY CREW OF MUSKETEER

RUN CODE	V _R KNOTS	α DEGREES	S,R RVD D	S,R RVD D	S,R RVD D	S,R RVD D	S,R RVD D	S,R RVD D	S,R RVD D	S,R RVD D	S,R RVD D	S,R RVD D	S,R RVD D
E-6A	110	45	14,4 4.6 0.1										
E-7A	110	45	6,2 NC 3.6	6,8 3.7 2.0									
F-1A,B	147	67.5	4,3 0.6 0.3	4,6 1.3 0	9,4 5.2 2.3	9,5 4.2 1.5	12,3 5.7 0.1	13,1 0.3 0.3					
F-7A	147	67.5	18,3 1.5 1.3										
G-1A	156	67.5	3,2 4.1 0.5	3,6 NC 0.5	17,5 NR 0.5	19,3 1.3 0.5							
G-2A	156	67.5	19,4 2.5 0.2										
G-7A	156	67.5	7,7 NC 1.6	7,8 NC 4.0	18,4 2.4 1.3								
H-1A	187	90	5,1 NC 0.3	5,2 1.7 0.3	9,8 NC 1.0	9,9 4.6 1.3	9,10 5.3 0.3	12,4 1.3 0.3	13,2 2.3 0.2	20,5 2.2 0.1	21,6 2.2 0.1		
H-5A	187	90	10,1 2.0 0.8										

TABLE 2B
DETECTION OF AZTEC BY CREW OF MUSKETEER

RUN CODE	V _R KNOTS	∠ DEGREES	S,R RVD D	S,R RVD D									
H-7A	187	90	7,9 3.6 1.2	7,10 NC 1.4									
I-1A	196	90	2,2 NC NR	2,5 NR NR	8,7 1.0 0	8,8 1.0 0.5	15,7 1.0 0.5						
I-7A	196	90	6,3 2.5 1.0	6,6 NC 1.7									
J-1A	219	112.5	5,3 0.4 0.3	5,4 6.6 0.5	12,1 1.0 0.5	17,6 2.5 0.5	19,5 2.5 0.8						
J-7A	219	112.5	9,11 2.2 2.0	16,5 6.5 0.7									
K-1A	229	112.5	3,3 3.2 0.5	3,7 3.2 0.3	13,3 1.2 0.9	13,4 0.6 0.5	17,7 2.5 1.0	17,8 4.0 1.5	19,7 5.0 0.8	19,8 4.0 1.2	20,6 1.5 1.0	21,8 1.7 0.2	
K-6A	229	112.5	7,1 2.3 1.6	7,2 3.7 1.4	11,2 1.4 1.4								
L-1A	243	135	4,2 0.5 0.3	4,5 NC 1.2	5,9 3.0 0.3	5,10 3.0 0.3	14,5 1.3 0.6	16,6 0.9 0.5					
L-7A	243	135	7,3 4.1 1.5	7,4 2.0 1.5	11,3 NC 2.5	11,4 3.5 NR	11,5 1.3 1.0						

TABLE 2C
DETECTION OF AZTEC BY CREW OF MUSKETEER

RUN CODE	V _R KNOTS	∠ DEGREES	S,R RVD D	S,R RVD D	S,R RVD D	S,R RVD D	S,R RVD D	S,R RVD D	S,R RVD D	S,R RVD D	S,R RVD D	S,R RVD D	S,R RVD D
M-1A	254	135	3,4 NC 0.3	16,7 3.5 1.0	18,5 NR 0.2	21,9 2.1 0.5							
N-1A	259	157.5	5,7 NC 1.0	5,8 1.5 0.9	8,3 0.5 0.3	8,4 0.5 0.2	12,2 3.6 1.2	13,5 2.7 1.1	13,6 2.9 0.9	19,6 2.0 0.2	21,10 3.0 0.2	22,3 1.5 0.3	22,4 2.2 0.2
O-1A	270	157.5	2,3 NR 0.5	8,5 1.0 0.3	8,6 0.3 0.2	20,1 1.6 0.2							
O-4A	270	157.5	6,4 NC 4.2	20,2 NC 0.9									
O-7A	270	157.5	20,3 NC 1.0										
O-8A	270	157.5	9,6 2.9 2.9	9,7 NC 4.5	12,5 3.9 3.6	12,6 NC 3.0							
Q-4A	275	180	9,2 2.1 2.1	9,3 5.1 3.1	22,5 4.1 0.5	22,6 3.6 0.4							

TABLE 2D
DETECTION OF AZTEC BY CREW OF MUSKETEER

RUN CODE	V _R KNOTS	α DEGREES	S,R RVD D	S,R RVD D	S,R RVD D	S,R RVD D	S,R RVD D	S,R RVD D	S,R RVD D	S,R RVD D
R-1A	325	120	11,8 5.2 0.5	11,12 6.7 1.1	15,1 7.3 0.3	15,2 6.6 0.6	15,4 7.5 0.3	15,5 7.0 0.5	20,7 6.2 0.3	20,9 5.6 0.4
R-4A	325	120	11,6 12.1 0.9	15,3 6.3 1.1	20,8 2.4 0.4					
S-1A	363	150	11,9 4.9 3.0	11,10 6.1 1.0	20,10 3.4 0.3					
S-2A	363	150	11,11 8.3 0.3	20,11 3.9 0.4						
S-5A	363	150	11,7 4.3 3.2							

TABLE 3

DETECTION OF GULFSTREAM BY CO-PILOT OF AZTEC

TABLE 4

P_D VS R FOR AZTEC DETECTION OF MUSKETEER

V _R - - 33 to 100 Knots α - - 0 to 45° (21 Data Points)		V _R - - 110 to 156 Knots α - - 45° to 68° (17 Data Points)		V _R - - 187 to 219 Knots α - - 90° to 113° (20 Data Points)		V _R - - 229 to 275 Knots α - - 113° to 180° (20 Data Points)	
Range	Pcd	Range	Pcd	Range	Pcd	Range	Pcd
8.9 nmi	0.048	6.7 nmi	0.059	9.9 nmi	0.050	5.5 nmi	0.050
8.0 nmi	0.095	6.0 nmi	0.118	7.6 nmi	0.100	4.8 nmi	0.100
7.7 nmi	0.143	5.2 nmi	0.177	4.3 nmi	0.150	4.3 nmi	0.150
6.3 nmi	0.191	5.0 nmi	0.235	4.1 nmi	0.200	4.0 nmi	0.250
6.1 nmi	0.238	4.3 nmi	0.294	3.8 nmi	0.250	3.7 nmi	0.300
5.9 nmi	0.286	4.0 nmi	0.353	3.7 nmi	0.300	3.0 nmi	0.350
3.8 nmi	0.381	3.8 nmi	0.412	3.5 nmi	0.350	2.3 nmi	0.400
3.7 nmi	0.476	3.7 nmi	0.471	3.3 nmi	0.400	2.2 nmi	0.450
3.4 nmi	0.523	3.6 nmi	0.530	3.1 nmi	0.450	1.9 nmi	0.550
3.1 nmi	0.571	3.1 nmi	0.588	3.0 nmi	0.550	1.6 nmi	0.600
3.0 nmi	0.619	2.9 nmi	0.647	2.9 nmi	0.600	1.5 nmi	0.650
2.9 nmi	0.666	2.5 nmi	0.765	2.6 nmi	0.700	1.3 nmi	0.700
2.8 nmi	0.761	1.9 nmi	0.882	2.3 nmi	0.750	1.2 nmi	0.800
2.5 nmi	0.810	0.9 nmi	1.000	2.1 nmi	0.800	1.0 nmi	0.950
2.0 nmi	0.905			2.0 nmi	0.850	0.5 nmi	1.000
1.8 nmi	0.951			1.8 nmi	0.900		
1.2 nmi	1.000			1.7 nmi	0.950		
				1.0 nmi	1.000		

TABLE 5
 P_D VS R FOR MUSKETEER DETECTION OF AZTEC

V_R - - 33 to 101 Knots α - - 0° to 45° (19 Data Points)	
Range	Pcd
8.5 nmi	0.053
6.5 nmi	0.105
6.0 nmi	0.211
5.6 nmi	0.263
5.1 nmi	0.316
4.8 nmi	0.368
3.9 nmi	0.421
3.8 nmi	0.474
3.4 nmi	0.526
2.4 nmi	0.631
2.3 nmi	0.684
2.1 nmi	0.737
1.8 nmi	0.790
1.5 nmi	0.895
1.3 nmi	1.000

V_R - - 110 to 187 Knots α - - 45° to 90° (23 Data Points)	
Range	Pcd
5.7 nmi	0.044
5.3 nmi	0.087
5.2 nmi	0.130
4.6 nmi	0.261
4.5 nmi	0.304
4.2 nmi	0.348
4.1 nmi	0.392
4.0 nmi	0.435
3.6 nmi	0.478
3.0 nmi	0.522
2.5 nmi	0.565
2.3 nmi	0.609
2.2 nmi	0.696
2.0 nmi	0.740
1.7 nmi	0.783
1.5 nmi	0.826
1.3 nmi	0.957
0.6 nmi	1.000

V_R - - 196 to 229 Knots α - - 90° to 113° (17 Data Points)	
Range	Pcd
6.6 nmi	0.059
6.5 nmi	0.118
5.0 nmi	0.176
4.0 nmi	0.294
3.7 nmi	0.353
3.2 nmi	0.470
2.5 nmi	0.706
1.7 nmi	0.765
1.0 nmi	1.000

V_R - - 243 to 275 Knots α - - 135° to 180° (18 Data Points)	
Range	Pcd
4.1 nmi	0.111
3.6 nmi	0.222
3.5 nmi	0.278
3.0 nmi	0.445
2.9 nmi	0.500
2.7 nmi	0.555
2.2 nmi	0.611
2.1 nmi	0.667
2.0 nmi	0.722
1.6 nmi	0.778
1.5 nmi	0.833
1.3 nmi	0.890
1.0 nmi	0.945
0.5 nmi	1.000

TABLE 6

P_D VS R FOR AZTEC DETECTION OF GULFSTREAM

V_R - - 325 to 363 Knots - - 120° to 150° (15 Data Points)	
Range	Pcd
12.1 nmi	0.067
8.3 nmi	0.133
7.5 nmi	0.200
7.3 nmi	0.267
7.0 nmi	0.333
6.7 nmi	0.400
6.6 nmi	0.467
6.3 nmi	0.533
6.2 nmi	0.600
6.1 nmi	0.667
5.6 nmi	0.733
5.2 nmi	0.800
3.9 nmi	0.867
3.4 nmi	0.933
2.4 nmi	1.000

TABLE 7

AIRCRAFT DIMENSIONS

AIRCRAFT	LENGTH	WINGSPAN
AZTEC	30 feet	37 feet
MUSKETEER	25 feet	33 feet
GULFSTREAM	80 feet	69 feet

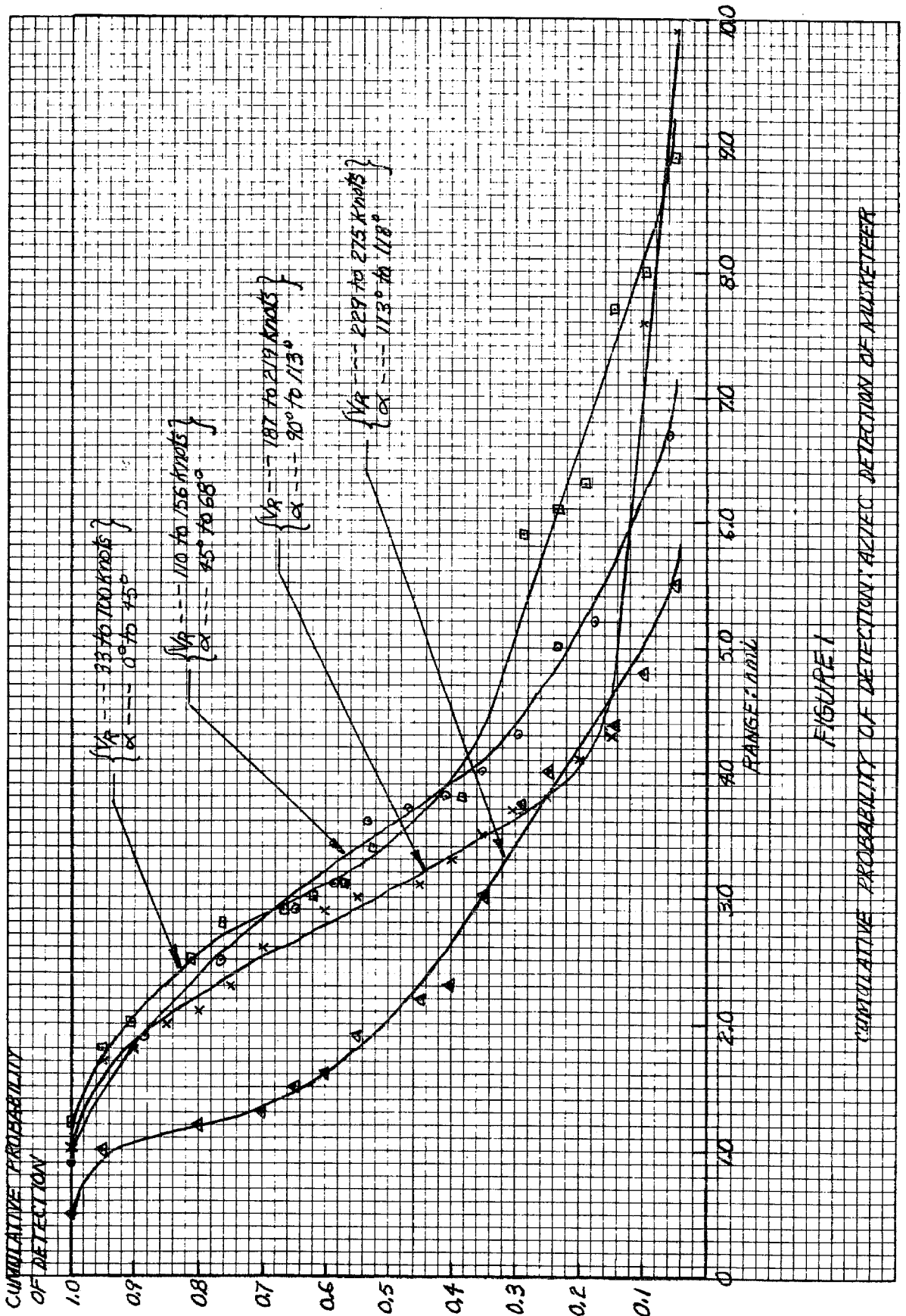
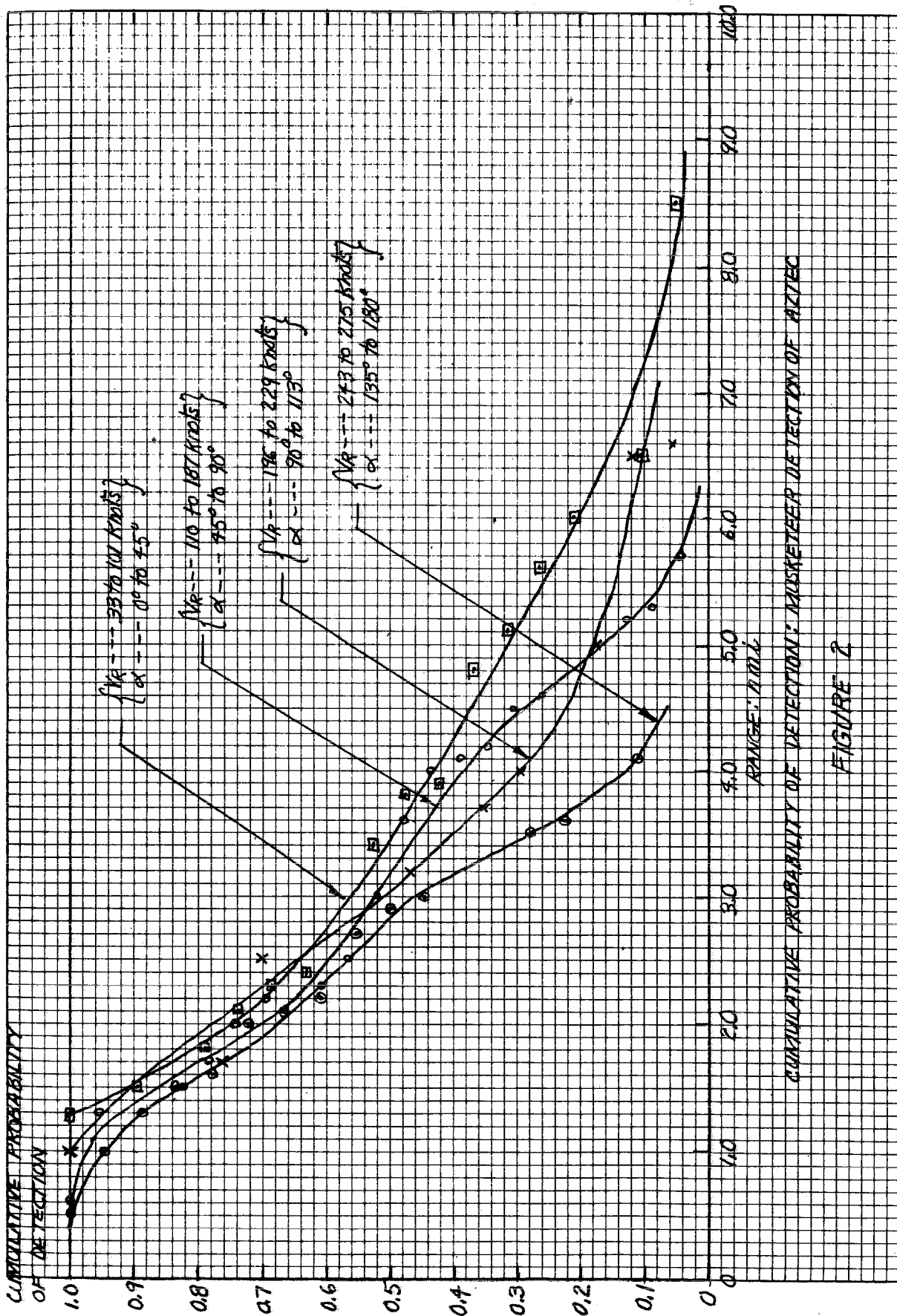
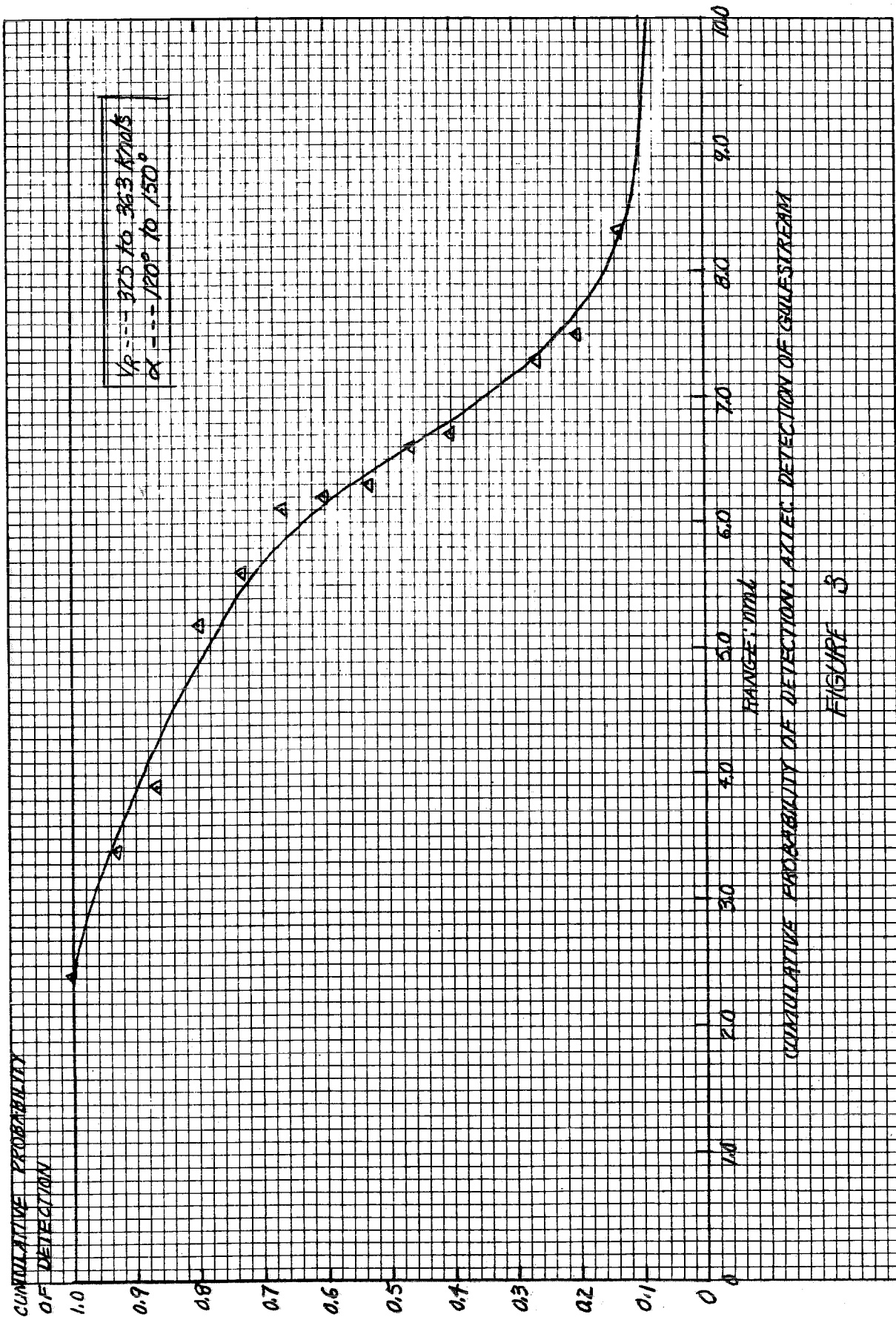


FIGURE 1
 CUMULATIVE PROBABILITY OF DETECTION, ALEFC DETECTION OF MURKETEER





CUMULATIVE PROBABILITY OF DETECTION ALLEGED DETECTION OF GULFSTREAM
 FIGURE 3

PART III

SUMMARY OF VISUAL DETECTION DATA
TAKEN DURING THE ATA/CAS FLIGHT TESTS

Contract No. DOT-FA-70WA-2263

Mr. W. Graham
Control Data Corporation

Submitted to:

Federal Aviation Administration
800 Independence Avenue
Washington, D. C.

Submitted by:

Control Data Corporation
Advanced Studies Laboratory
4201 Lexington Avenue North
St. Paul, Minnesota

Date: 1 May 1972

Author: W. Graham

SUMMARY OF VISUAL DETECTION DATA
TAKEN DURING ATA/CAS FLIGHT TESTS

Introduction

During the last few weeks of flight testing of the ATA/CAS equipments by the Martin Marietta Corporation, the FAA supplied observers to record data concerning the range of visual detection. Because of the near-collision geometry of the runs and the presence of the CAS equipment, which gave a precise measure of the range between the aircraft, these tests were an ideal opportunity to make such observations. Details of the equipment flown and a summary of each flight are given in Reference 1.

In the interest of safety no runs were made when the air-to-air visibility was estimated to be less than five miles and indeed, out of a total of 43 runs observed, the range from the observer's aircraft at first visual detection exceeded five nautical miles 79% of the time. One would infer from this that first detection occurred in one or both aircraft 96% of the time beyond this range.

Each run was designed to test some feature of the CAS equipment. Four aircraft were involved, and they flew a wide range of speeds and relative headings, producing a range of closing speed from 50 to 900 knots. The runs were conducted at small altitude differences, in order to produce CAS alarms.

Geometrical Considerations

Since the range at first detection is expected to be a function of closing speed, an estimate of the closing speed was made for each run. There were three different ways (potentially) of making this estimate; not every way was available in every run. Figure 1 illustrates the source of these estimates. The diagram on the left represents the observer's aircraft at point O and the intruding aircraft on a relative track from point A to point C, moving with the relative velocity V_r , and passing at a distance of closest approach d . Nominally the runs are set up for $d = 0$, but in practice the miss is considerable; the minimum separation was not recorded.

The diagram on the right in Figure 1 illustrates the range/time history of a typical run with a finite miss d . If d were zero V_r would pass through 0 and the range rate would be constant over the run and equal to V_r . If $d \neq 0$ the range rate decreases as the point of closest approach C is neared, reaching zero range rate at point C . At ranges large compared with d there is little difference between the actual closing speed and V_r ; the nominal V_r was recorded in almost every run but it can be expected to deviate from the actual value because of differences in actual speeds and headings from the nominal values. This nominal value of V_r is one of the three estimates of range rate available.

The CAS is designed to alert the pilot to prepare to climb or descend at the so called tau 2 warning time defined by the relationship:

$$\tau_2 = \frac{R_p - R_o}{\dot{R}_p}$$

During the runs observed τ_2 was set to 30 seconds, and R_o was set to 1.6 nmi. Solving for the range rate \dot{R} :

$$\dot{R}_p = (R_p - 1.6) \times 120 \text{ knots}$$

R_p is the range at which the τ_2 alarm is triggered.

It can be seen from Figure 1 that the range rate \dot{R}_p can be expected to be somewhat less than V_r depending on d and R_p . It is also subject to errors in its measurement by the CAS equipment, but it affords a second estimate of the closing speed in each run.

The CAS is designed to generate a command for climb or descend at the so called tau 1 warning time defined by the relationship:

$$\tau_1 = R_c / \dot{R}_c$$

During the runs observed τ_1 was set to 25 seconds. This provides a third estimate of closing speed:

$$\dot{R}_c = R_c \times 144 \text{ knots.}$$

The tau 1 and tau 2 alarms can also be triggered if the range between the aircraft is less than 0.6 and 2.3 nmi respectively. In that event the range rate is less than that

calculated from the above equations. During the observations made, the range alarm was only triggered when the indicated range rate was in the lowest speed interval so that the distinction between a range alarm and a τ alarm has no effect on the data reduction.

The Data

Table I summarizes the observations which were made. Generally the pilot or co-pilot was the first to observe the target; occasionally the observer did so. The range at visual detection, R_v , which appears in the Table, is the range at which the target was first sighted by any of these three people. In some cases only the nominal relative velocity was recorded; in others all three estimates of closing speed are available. Generally the three estimates decrease in magnitude in the expected order: V_r , \dot{R}_p , \dot{R}_c . The estimate \dot{R}_p was always used when it was available since the range R_p is generally closer in magnitude to the range R_v than was the range R_c , and hence gives a better estimate of the closing speed at the range of visual detection and beyond it. The closing speed selected for sorting the data is indicated by an asterisk in the tabulation for each run.

Four different aircraft appeared as targets during the runs. These are identified by three numbers (from the N number); the type is given in a footnote to the Table. The wingspan and length of these aircraft are given in Figure 2.

There were only five runs with either of the two jet aircraft as target at closing speeds below 460 knots and only one run with a 404 target at a closing speed above 400 knots. These runs have been eliminated in order not to confound target size and closing speed. The runs were all planned without regard to the angle of the sun with respect to the line of sight from the observer to the target.

The results are summarized in Figure 2, which also gives some of the results of analysis of sightings made during the recent FAA/CDC photographic flight test program reported in Reference 2. The two curves summarizing sightings of the 404 aircraft in the 50 - 200 knot and 200-400 knot closing speed

intervals do not show a significant speed dependence. The sightings of the two jet aircraft, all in the 460 - 900 knot closing speed interval, were at significantly shorter ranges than the 404 sightings showing a combined effect of target size and closing speed (and also target aspect).

The data reported in Reference 2 were taken under somewhat different conditions. With the Gulfstream and Musketeer targets the sightings were made by one observer who had no task other than the detection of the target; other crew members said nothing if they detected the target first. The runs were planned, for photographic reasons, so that the sun was always behind the observer. In the runs with the Aztec as target, detections were made sometimes by a pilot alone in the observing aircraft (a Musketeer), and on other occasions either by the pilot or by an observer in the co-pilot's seat. The sun was within his field of view.

The sightings of the Gulfstream compare remarkably well with the sightings of the 404 aircraft, the differences in size and speed being small. The data for the Aztec and Musketeer targets show detection ranges of about half of those recorded with the larger Gulfstream and 404 targets.

Discussion

All these data were taken under conditions of good visibility at a time when the observers knew they were in a near-collision encounter with the target aircraft. During the ATA/CAS tests the range to the target was available. In all the tests summarized in Figure 2 the observers knew approximately the relative bearing at which the target would first become visible. It is impossible to give a firm estimate of what the uncertainty in angle was. If the range at first detection was short, of the order of the miss distance, the relative bearing could be considerably removed from what it was at the beginning of the run. Such experiences would have the effect of expanding the field of search on subsequent runs. Our guess is that the effective width of field was something like $\pm 25^\circ$.

With the exception of nose-to-nose encounters with jet aircraft the target was always detected, and when detected, there were more than 10 seconds to closest approach in about 99% of the runs with small targets and 100% of the runs with larger targets. These results show conclusively the significant potential of PWI devices when compared with Howell's data taken with pilots who did not know they were flying collision courses (Reference 3); see also Ref.4 for other closing speeds.

In conditions of poorer visibility and greater workload in the cockpit the results might show considerable room for improvement. For this reason we hesitate to conclude that the data supports the finding that the presumed accuracy in relative bearing is adequate.

References

1. "Collision Avoidance System, Flight Test and Evaluation Program", Vol. II Final Report April 1970 Prepared for the Air Transport Association by the Martin Marietta Corporation, Baltimore, Maryland 21203
2. Lyons, J. "Summary of Visual Detection Data" (of FAA/CDC photographic flight tests), Report No. CDC-JL-5 March 1972 Contract No. DOT-FA70WA-2263
3. Howell, W. "Determination of daytime conspicuity of transport aircraft", CAA TDC, Tech. Develop. Report 304, May 1957
4. Graham, W. and Orr, R.H., "Separation of Air Traffic by Visual Means: An Estimate of the Effectiveness of the See and Avoid Doctrine" Proc. IEEE 58 3 March 1970

SUMMARY OF VISUAL DETECTION DATA TAKEN DURING ATA/CAS FLIGHTS

Date (1969)	Run No.	Target A/C	R _p nmi	R _p knots	R _c nmi	R _c knots	R _v nmi	V _r knots		
27 Oct.	3	121					6.1	244*		
	4						5.2	460*		
	5						4.0	746*		
	6						5.0	900*		
	7						7.4	100*		
	8						11.3	244*		
	9						6.2	460*		
	11						-	900*		
	29 Oct.		1	432	3.2	192*			7.7	333
			3		3.4	212*			6.2	333
			5		3.7	248*	1.3	190	6.1	333
6		3.8	259*		2.0	208	8.6	333		
7		2.9	151*		1.6	223	13.3	255		
8		3.7	253*		1.5	218	5.6	255		
10		6.7	612*		4.9	706	6.7	575		
31 Oct.	1	121					5.7	900*		
	2		3.3	204			3.3	244		
	3		7.4	835*	1.3	189	5.6	460		
	4		6.4	580*	3.4	494	6.1	750		
	7		5.1	420*	2.0	288	7.5	460		
	8		7.0	648*	3.4	490	2.6	750		
	1'		7.8	743*	5.7	820	-	900		
	2'		2.9	156*	1.1	151	3.9	244		
	6'		2.8	140*			4.1	245		
	7'		4.7	372*	2.3	334	6.1	640		
	8'		6.3	564*	3.9	562	12.4	750		
10 Nov.	2	427	2.6	120*	1.1	158	7.5			
	3		2.9	156*	1.1	158	7.5			
	4		2.6	120*	0.8	115	5.2			
	5		4.0	346*	2.0	288	7.5			
	6		2.4	96*			5.2			
	7		2.6	120*	1.4	200	7.5			
	8		3.7	252*	2.1	302	4.0			

TABLE I

VISUAL DETECTION DATA (continued)

Date	Run No.	Target A/C	R_p	\dot{R}_p	R_c	\dot{R}_c	R_v	V_r
11 Nov.	1	427					6.6	50*
	2						5.7	175*
	3		2.3	84*			3.9	175
	4		2.8	144*			10.6	175
	5		3.2	196*			10.0	175
	6		2.6	120*	0.9	130	8.7	175
	7		2.2	72*			3.0	175
	8		3.0	168*	1.5	214	10.5	425
	9		4.1	298*	1.6	230	12.1	425
	10							12.8

NOTES:

Target aircraft

242 Jet Falcon
 121 Jet Star
 427 Martin 404
 432 Martin 404

R_p range at tau 2 alarm,
 (prepare to climb/descend)
 R_c range at tau 1 alarm
 (climb/descend)
 R_v range at visual detection
 V_r nominal relative velocity
 magnitude

$\dot{R}_p = (R_p - 1.6)_{\text{nmi}} \times 120$ indicated closing speed in knots at
 tau 2 alarm (if $R_c > 2.3$ nmi)

$\dot{R}_c = 144 \times R_c$ (if $R_c > 0.6$ nmi)
 indicated closing speed in knots at
 tau 1 alarm

TABLE I (continued)

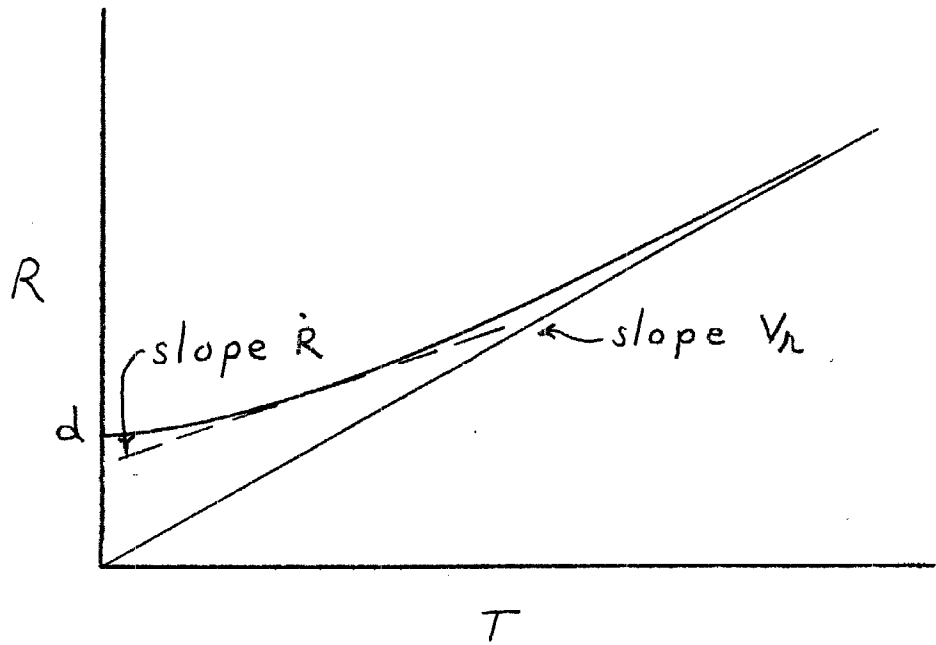
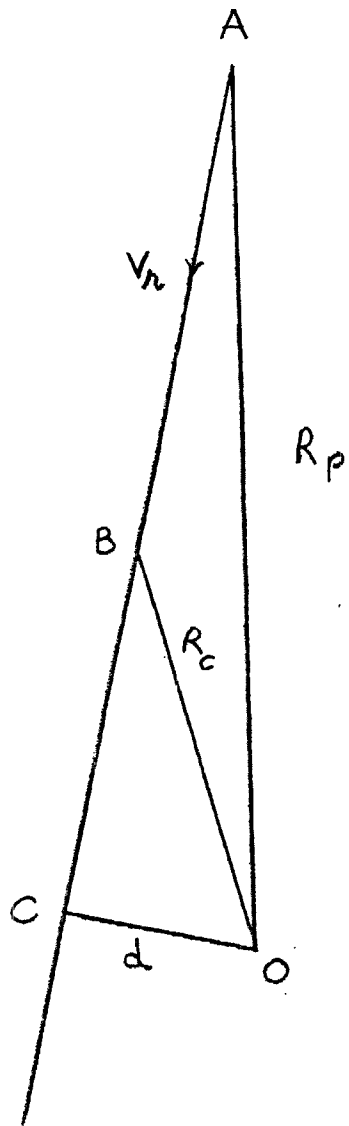
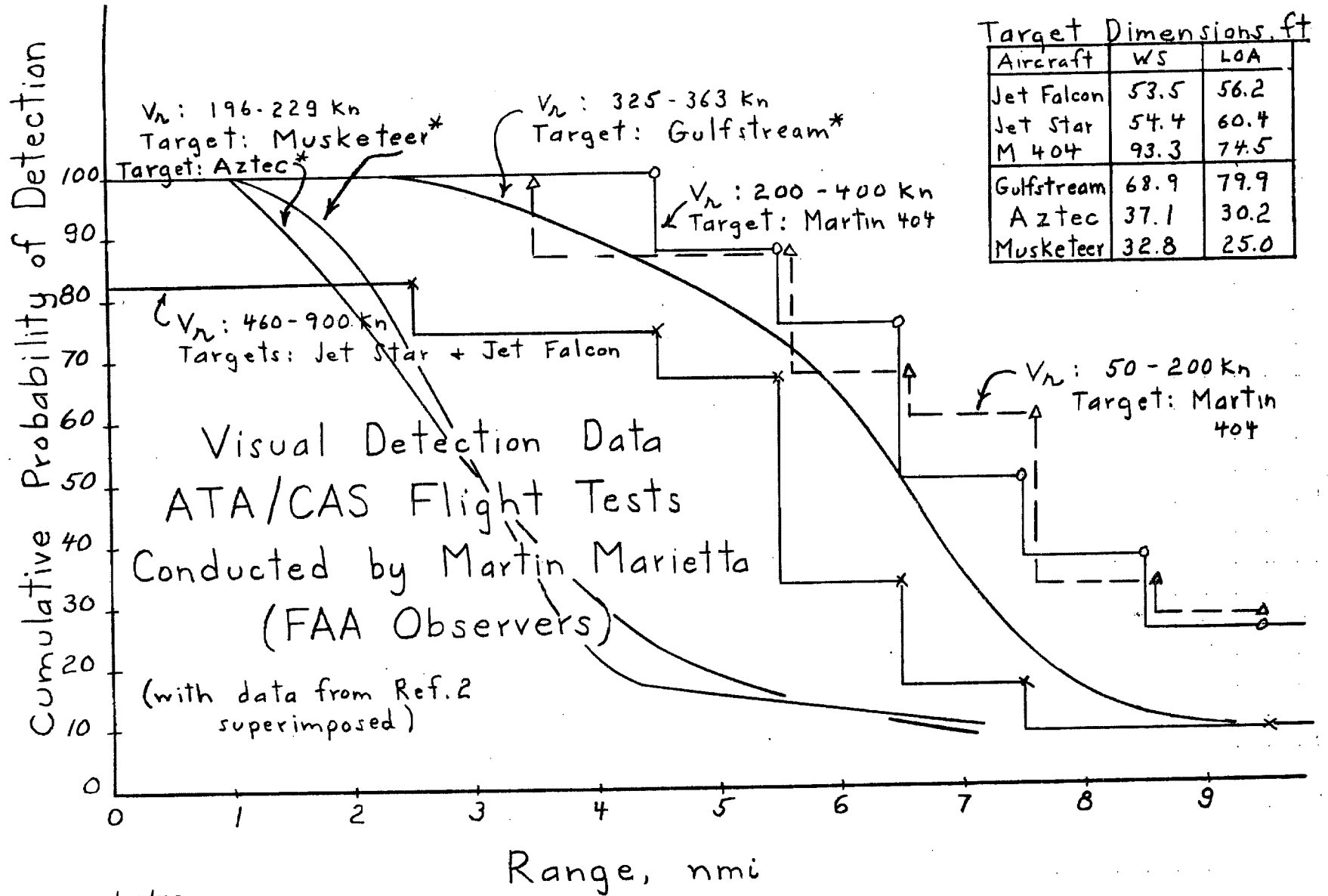


Figure 1



4/16/72
wg

* Data from Ref. 2

Figure 2